Journal of
Ceramic Science
and Technology

J. Ceram. Sci. Technol., **12** [1] 59-62 (2021)
DOI: 10.4416/JCST2020-00024
available online at: http://www.ceramic-science.com

Short Communication

A Polishing-Free Etching Method for Microstructure Observation of Fine-Grained Ceramics

M. Liu[1, 2, 4], J. Zhao[2], S. Shimai[2], J. Zhang[*1, 2, 3], H. Chen[2, 4], H. Chen[2], D. Han[2], J. Liu[2], S. Wang[*1, 2]

[1]State Key Laboratory of High Performance Ceramics and Superfine Microstructure, Shanghai Institute of Ceramics, Chinese Academy of Sciences, Shanghai 200050, China.
[2]Key Laboratory of Transparent Opto-functional Inorganic Materials, Shanghai Institute of Ceramics, Chinese Academy of Sciences, Shanghai 201899, China.
[3]Center of Materials Science and Optoelectronics Engineering, University of Chinese Academy of Sciences, Beijing 100049, China.
[4]University of Chinese Academy of Sciences, Beijing 100049, China

received November 19, 2020; received in revised form February 2, 2021; accepted February 6, 2021

Abstract

Microstructural studies are very important because of their decisive role in the properties of advanced ceramics. During the sample preparation process, it is critical to grind, polish, and etch the fracture surface of the ceramic for effective microstructure observation. Here, a sample preparation process is proposed based on direct etching of the fracture surface of the ceramic without the time-consuming grinding and polishing. We used this method to create micrographs for $MgAl_2O_4$, Al_2O_3, and ZrO_2 ceramics with an average grain size less than 1 µm; these were clearly resolved by SEM. More importantly, the damage resulting from grinding or polishing is minimized, and SEM images taken of samples prepared with this method are closer to the original morphology of the microstructures. This method also greatly simplifies the sample preparation process and is especially suitable for fine-grained ceramics.

Keywords: Fracture surface, ceramics, etching, SEM

I. Introduction

The microstructure of ceramics includes grains, inclusions, pores, and grain boundaries [1,2]. To obtain ceramics with excellent properties, the first goal is to determine the relationship between the microstructure and properties of advanced ceramics. Usually, to effectively resolve the microstructure of ceramics, high-quality sample preparation processes are necessary before SEM observation.

Traditionally, the fracture surface or the polished surface after etching has been chosen for microstructure observation. The contrast between grains and grain boundaries is easily distinguished for a ceramic that fractures in a transgranular fracture mode. If the roughness of the fracture surface is relatively low, then observing the fracture surface is enough to obtain the microstructure morphology [3,4]. However, if the roughness of the fracture surface is high – especially when the grain size is larger than the depth of field (DOF) of the microscope, the microstructure morphology cannot be imaged successfully. In this case, post-processing steps including grinding, polishing, and etching must be carried out on the fracture surface to obtain a flat surface with sufficient contrast between the grains and grain boundaries.

For a ceramic that fractures in the intergranular fracture mode, the contrast between the grains and grain boundaries cannot be easily distinguished on the fracture surface owing to the existence of glassy phases and impurities segregated on grain boundaries. In this case, similar post-processing steps, including grinding, polishing, and etching, are needed for successful imaging [5–7]. However, during the grinding and polishing processes, the practical morphology of the microstructure can be somehow destroyed [8–10]. Lateral cracks and grain pullout resulting from the machining processes are barriers to detecting detailed information on the microstructure. Although newly developed advanced polishing technologies, such as mechanical polishing [9], chemical polishing [11], or ion-beam polishing [12], can sharply minimize the destruction of the original microstructure of ceramics, extensive hands-on experience is still needed to properly prepare high-quality samples.

With the development of fine-grained ceramics, surface flaws such as lateral cracks or grain pullout are much

* Corresponding author: jianzhang@mail.sic.ac.cn; swwang51@mail.sic.ac.cn

more serious than that in coarse-grained ceramics during the machining process. Residual polishing particles may even hide the practical information of grains or pores. The methods mentioned above for observing the microstructure of ceramics on the fracture surface or the polished and etched surface are not suitable for fine-grained ceramics. Advanced ceramics with grain sizes on the submicron scale or lower can be easily fabricated. As a result, the surface roughness that results from the fractured surface of the fine-grained ceramics is small enough to be ignored for microscopic imaging on submicron scale. In other words, the grain size of advanced ceramics is much smaller than the DOF of microscopes. High-quality micrographs can thus be obtained successfully. Hence, the fracture surface of fine-grained ceramics is sufficient to be effectively imaged after proper etching. However, the method for observing the microstructure of a fine-grained ceramic based on direct etching of the fracture surface has seldom been used before [13].

In this paper, we have demonstrated the feasibility of a simple method for observing the microstructures of fine grain ceramics by comparing the standard polishing-etching method and the direct etching method. The thermal etching processes are applied directly on the fracture surfaces of $MgAl_2O_4$, Al_2O_3, and ZrO_2 ceramics respectively. Abundant microstructural information has been obtained from the SEM images taken of these etched fracture surfaces.

II. Materials and Method

Both $MgAl_2O_4$ and Al_2O_3 powders were provided by Baikowski, France. ZrO_2 powder was provided by Tosoh, Japan. The average particle sizes (D50) of $MgAl_2O_4$, Al_2O_3, and ZrO_2 powder were 330 nm, 370 nm, and 220 nm, respectively. These were all tested with a laser particle size analyzer (Master Sizer 2000, Malvern, UK). Ceramics of both $MgAl_2O_4$ and Al_2O_3 were formed by means of gel-casting with Dolapix CE64[14] and PIBM gelling system, respectively [15, 16]. The ZrO_2 ceramic was formed by means of cold isostatic pressing at 200 MPa. After formation, the ceramics were heated to 800 °C to burn out the binder and then sintered in air at different temperatures for densification. The ZrO_2 ceramic was post-HIP treated at 1 260 °C for 3 h at 200 MPa argon pressure. The processing conditions of all of the three ceramics are listed in Table 1. The fracture surfaces were thermally etched for SEM observations. The thermal etching temperatures of $MgAl_2O_4$, Al_2O_3, and ZrO_2 ceramics were 1 200 °C, 1 000 °C, and 1 000 °C, respectively. For comparison, the just-fractured surfaces without etching were observed along with the thermally etched surfaces after polishing. The polishing process was performed using 6 µm and 2 µm diamond slurries. The micrographs were all obtained with field emission scanning electron microscopy (FE-SEM, SU9000, Hitachi, Japan).

III. Results and Discussion

Fig. 1 shows the microstructure of the $MgAl_2O_4$ ceramic sintered at 1 500 °C for 3 h. Panels include micrographs of the fracture surface (a) and thermally etched fracture surfaces (b) and (c). In Fig. 1 (a), the fracture surface is almost flat with no contrast between the grains and grain boundaries. Obviously, the as-sintered $MgAl_2O_4$ ceramic fractured in an intergranular fracture mode. Traditionally, polishing and etching processes are required for ceramics fractured in this mode before the microstructure is observed. However, in this process, machining by means of grinding or polishing was not needed owing to the previously formed flat surface after fracturing. In Fig. 1 (b) and (c), clear

Table 1: Preparation processes for $MgAl_2O_4$, Al_2O_3, and ZrO_2 ceramics

Powder	Company	Forming process	Sintering temperature (°C)	Etching temperature (°C)	Etching time (h)
$MgAl_2O_4$	Baikowski S25CR	Gel-casting	1 500	1 200	3
Al_2O_3	Baikowski SMA6	Gel-casting	1 400	1 000	3
ZrO_2	Tosoh Zpex	CIP (200 MPa)	1 400 (pre-sintering) 1 260 (HIP)	1 000	3

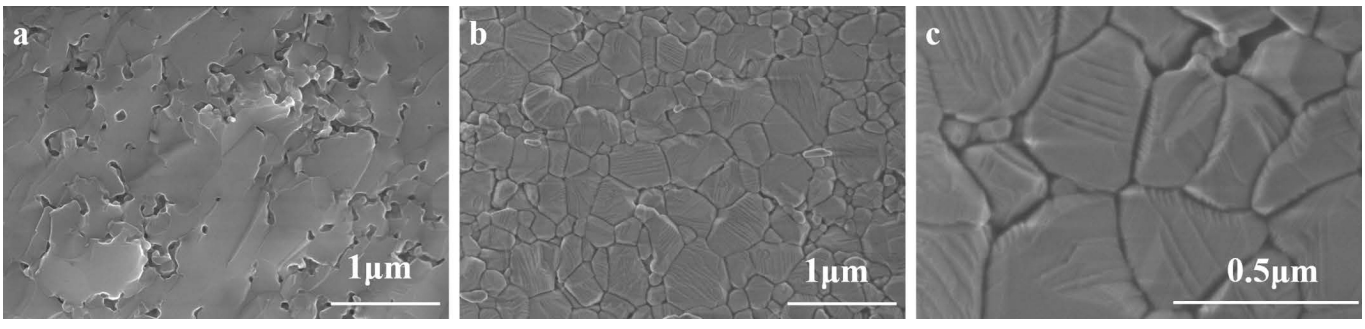

Fig. 1: Micrographs of $MgAl_2O_4$ ceramics. (a) Fracture surface; (b) and (c) Thermally etched fracture surfaces.

grain boundaries can be distinguished after directly thermal etching of the fractured surface. Grain sizes were distributed on a scale of 50 – 500 nm; all were imaged successfully. The original pores after etching are still similar to those in Fig. 1 (a). In summary, the as-prepared fine-grained $MgAl_2O_4$ ceramic described here has grains small enough to be totally imaged on the micrometer scale by means of SEM. As a result, the machining step was diminished, and the etching process proceeded directly on the fracture surface. The simplified sample preparation method is not only time-saving but can also protect the original microstructure from damage during machining.

In contrast, if machining processes such as grinding or polishing are performed, then destruction such as scratches and pullout grains may occur. Fig. 2 shows the three typical types of destruction on the microstructure of the $MgAl_2O_4$ ceramic that resulted from polishing and etching. Surprisingly, Fig. 1 and Fig. 2 show SEM images taken of the same sintered $MgAl_2O_4$ ceramic, but they appear completely different. In Fig. 2 (a) and (b), many grains as small as 30 nm or less are shown. However, the actual grain sizes are distributed between 50 nm and 500 nm. As against the same ceramic sample shown in Fig. 1, it can be seen that the machining and etching processes on the ceramic surface in Fig. 2 resulted in some misleading phenomena such as ultra-small grains. Abrasive particles might be left on the ceramic surface after polishing.

Fig. 2 (b) shows obvious scratches that resulted from grinding. These affect the imaging quality and the calculated average grain size. Fig. 2 (c) shows a single pore with a size of about 1 µm. This is several times bigger than the average grain size. During grinding and polishing, some grains may be pulled out owing to weak grain boundaries; the pore-like information is then detailed on the SEM image. The large pore in Fig. 2 (c) may result from grain pullout during machining. These types of damage (false ultra-small grains, scratches, etc.) are barriers to researchers and obscure the true features of the ceramic microstructure.

For a ceramic that fractures in the transgranular fracture mode, observing the fracture surface is preferred for obtaining the actual original morphology of the microstructure. No etching process is usually necessary owing to the contrast between the grains and the grain boundaries that already exist because the fracturing behavior occurs just along the grain boundaries. Glassy phases and impurities may exist on the grain boundaries of these ceramics. This will also affect the imaging quality of SEM. To increase contrast, the grain boundaries can be grooved with an etching process on the fracture surface before observation. The microstructure can be of higher quality after etching.

Fig. 3 (a) shows the thermally etched fracture surface of the ZrO_2 ceramic. No pore can be identified here because the ZrO_2 ceramic was pre-sintered first, and then HIPed at 1 260 °C for 3 h with 200 MPa argon pressure. The ceramic was fully densified. The grain boundaries after grooving by means of thermal etching are more distinct than without etching [Fig. 3 (b)]. Comparing the two micrographs from the different pre-processing steps suggests that although the etched fracture surface shows better contrast, it somehow changes the original state of the fracture surface. Clearly, the edges and corners of the grains in Fig. 3 (a) have been erased by thermal etching. Nevertheless, the micrographs obtained from the fracture surface with or without etching processes were better than Fig. 3 (c), which resulted from polishing and etching processes. Although it seems that no obvious destruction occurred on the microstructure of the ZrO_2 ceramic, some white impurities do remain on the surface. In summary, the etching process on the fracture surface may not be necessary for ceramic fractures just along the grain boundaries or in cases with clear grain boundaries.

However, not all ceramics fractured in a transgranular mode show clear contrast between the grains and grain boundaries. In this case, proper etching processes are necessary before SEM observation. For example, the alumina ceramic fractures in a transgranular fracture mode, but the contrast between the grains and grain boundaries is low. Fig. 4 (a) and (b) show SEM images of an as-fractured surface without etching and a thermally etched fracture surface of the alumina ceramic, respectively. Obviously, the pores observed from Fig. 4 (a) and (b) are very similar. Fig. 4 (b) shows better contrast between the grains and grain boundaries owing to the glassy phases or impurities that have been erased by etching.

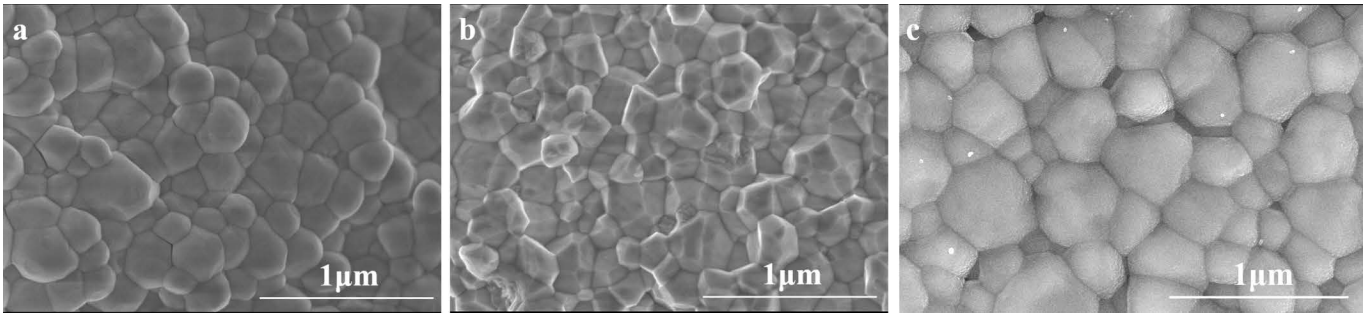

Fig. 3: Micrographs of ZrO_2 ceramics. (a) Thermally etched fracture surface; (b) As-fractured surface; (c) Polished and thermally etched surface.

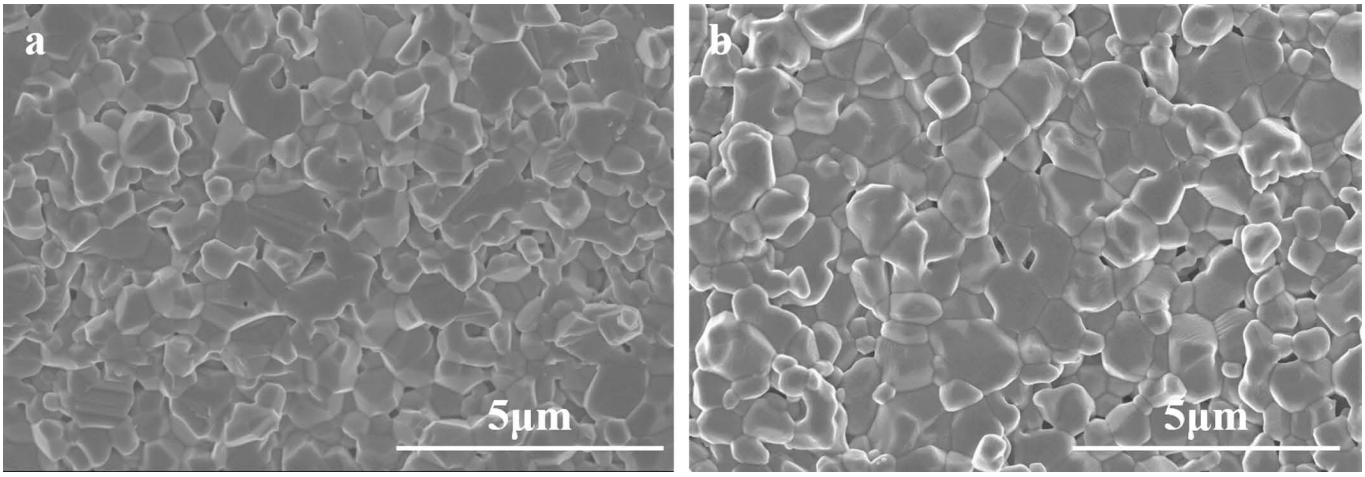

Fig. 4: Micrographs of Al_2O_3 ceramics. (a) As-fractured surface; (b) Thermally etched fracture surface.

VI. Conclusions

A practical method that directly etches the fracture surfaces instead of etching the polished surfaces is more convenient for SEM sample preparation. More importantly, the microstructure close to the original fracture surface can be detected instead of possible misguiding information owing to the destruction that has occurred during the machining process. This proposed method is especially suitable for fine-grained ceramics.

Acknowledgements

This work was supported by the National Natural Science and Foundation [grant number 51772309]; Scientific Instrument Developing Project of the Chinese Academy of Sciences [grant number YJKYYQ20180042] and the Natural Science Foundation of Shanghai [grant number 19ZR1465000].

References

1 Kingery, W.D., Bowen, H.K., Uhlmann, D.R.: Introduction to ceramics, 2nd edition. John Wiley & Sons, Inc., New Jersey, 1976.

2 Krell, A., Hutzler, T., Klimke, J. Potthoff, A.: Fine-grained transparent spinel windows by the processing of different nanopowders, *J. Am. Ceram. Soc.*, **93**, 2656 – 2666, (2010).

3 Chen, H., Shimai, S., Zhao, J., Di, Z., Mao, X., Zhang, J., Liu, J., Zhou, G., Wang, S.: Pressure filtration assisted gel casting in translucent alumina ceramics fabrication, *Ceram. Int.*, **44**, 16572 K – 16576, (2018).

4 Zhou, Y., Hirao, K., Yamauchi, Y., Kanzaki, S.: Densification and grain growth in pulse electric current sintering of alumina, *J. Eur. Ceram. Soc.*, **24**, 3465 – 3470, (2004).

5 Zum Gahr, K.-H., Bundschuh, W., Zimmerlin, B.: Effect of grain size on friction and sliding wear of oxide ceramics, *Wear*, **162**, 269 – 279, (1993).

6 Sun, Y., Qin, X., Zhou, G., Zhang, H., Peng, X., Wang, S.: Gelcasting and reactive sintering of sheet-like YAG transparent ceramics, *J. Alloy. Compd.*, **652**, 250 – 253, (2015).

7 Owate, I.O., Freer, R.: Thermochemical etching method for ceramics, *J. Am. Ceram. Soc.*, **75**, 1266 – 1268, (1992).

8 Luo, J., Dornfeld, D.A.: Material removal mechanism in chemical mechanical polishing: theory and modeling, *IEEE T. Semiconduct M..*, **14**, 112 – 133, (2001).

9 Xu, W., Lu, X., Pan, G., Lei, Y., Luo, J.: Ultrasonic flexural vibration assisted chemical mechanical polishing for sapphire substrate, *Appl. Surf. Sci.*, **256**, 3936 – 3940, (2010).

10 Xie, Z.-H., Moon, R.J., Hoffman, M., Munroe, P., Cheng, Y.-B.: Role of microstructure in the grinding and polishing of α-sialon ceramics, *J. Eur. Ceram. Soc.*, **23**, 2351 – 2360, (2003).

11 Łyczkowska, E., Szymczyk, P., Dybała, B., Chlebus, E.: Chemical polishing of scaffolds made of Ti-6Al-7Nb alloy by additive manufacturing, *Arch. Civ. Mech. Eng.*, **14**, 586 – 594, (2014).

12 Chkhalo, N.I., Churin, S.A., Pestov, A.E., Salashchenko, N.N., Vainer, Y.A., Zorina, M.V.: Roughness measurement and ion-beam polishing of super-smooth optical surfaces of fused quartz and optical ceramics, *Opt. Express*, **22**, 20094 – 20106, (2014).

13 Shan, J., Li, C., Wu, J., Liu, J., Chen, A., Shi, Y.: Sintering behavior and microstructural evolution of the monodispersed β-gallium oxide micro-particles with different morphology and size, *Ceram. Int.*, **43**, 16843 – 16850, (2017).

14 Liu, M., Shimai, S., Zhao, J., Zhang, J., Han, D., Li, Y., Liu, J., Wang, S.: Gel-casting of $MgAl_2O_4$ transparent ceramics using a common dispersant, *J. Am. Ceram. Soc.*, **102**, 3081 – 3084, (2019).

15 Yang, Y., Shimai, S., Sun, Y., Dong, M., Kamiya, H., Wang, S.: Fabrication of porous Al_2O_3 ceramics by rapid gelation and mechanical foaming, *J. Mater. Res.*, **28**, 2012 – 2016, (2013).

16 Yang, Y., Shimai, S., Wang, S.: Room-temperature gelcasting of alumina with a water-soluble copolymer, *J. Mater. Res.*, **28**, 1512 – 1516, (2013).